LOGIC (JOURNAL ENGINEERING DESIGN AND TECHNOLOGY)

Journal Engineering Design and Technology
Vol. 26 No.2 July 2026 ; p. 120 - 132
Journal Homepage : http://ojs2.pnb.ac.id/index.php/LOGIC
p-ISSN : 1412-114X e-ISSN : 2580-5649

Design of a Fuzzy Logic Based Control System for BLDC Motor Speed and Cooling Fan Using Error and Error Change

Aulia Adawiyah [1)*], Arief Suryadi Satyawan [2)], Helfy Susilawati [1)], Esti Fitria Wulandari [1)], Rendi Tri Sugian [1)], Iasya Faiqoh Nurrohmah [1)], Fajar Rahmat Akbar [1)], Andika Muhammad Nur Kholiq [1)]

1) Departement of Electrical Engineering, Garut University, Garut, Indonesia
2) Telecommunications Research Center, National Research and Innovation Agency (BRIN), KST Samaun Samadikun, Bandung, Indonesia

Corresponding email [1)*] : 24052122002@fteknik.uniga.ac.id

Abstract. This study presents the design and simulation-based evaluation of a fuzzy logic controller for a 48 V, 10 kW BLDC motor system integrating speed control and thermal management through a cooling fan. The controller employs four input variables, namely RPM error, change in RPM error, temperature error, and change in temperature error, within an 81-rule fuzzy inference system using triangular membership functions. Minimum-based rule evaluation, maximum aggregation, and weighted-average defuzzification are applied to generate PWM control signals. An interactive GUI-based simulation platform incorporating visualization, data logging, and automated testing was developed to systematically evaluate the complete fuzzy rule base. Simulation results from all 81 fuzzy-rule combinations show that the motor PWM adapts to variations in speed error, while the fan PWM is prioritized under elevated temperature conditions to enhance thermal safety. Overlapping membership functions produce smooth intermediate PWM outputs, whereas the discrete PWM-to-RPM mapping results in stepwise speed variations. Overall, the proposed controller demonstrates stable and adaptive speed and thermal control behavior in simulation and provides a practical foundation for future real-time hardware implementation and quantitative experimental validation.

Keywords : Fuzzy control, BLDC motor, Speed control (RPM), Temperature control / fan control.

1. INTRODUCTION

The development of control systems in electrical engineering and mechatronics requires controllers that are stable, adaptive, and robust under dynamically changing operating conditions. In BLDC motor systems, one of the main challenges is maintaining the desired RPM despite load variations, voltage fluctuations, and external disturbances, while also managing the thermal condition of the motor during high-speed and high-power operation. Uncontrolled temperature rise can reduce efficiency, accelerate insulation degradation, and shorten motor lifespan. Therefore, thermal management is an essential aspect of motor control that cannot be separated from speed regulation [1]. Conventional controllers such as PID are still widely used in industrial applications because of their simple structure. However, their performance strongly depends on the accuracy of the mathematical model and the parameter tuning process [2]. Since BLDC motors and cooling systems are nonlinear, time-varying, and influenced by load and environmental conditions, model-based controllers may suffer from overshoot, oscillations, or significant steady-state error when operating outside nominal conditions [3].

Fuzzy logic has emerged as an effective approach for controlling nonlinear and uncertain systems because it can handle nonlinearities and uncertainties without relying entirely on precise mathematical models. Instead, fuzzy logic controllers employ linguistic IF–THEN rules to represent heuristic knowledge, making them well suited for systems operating under varying and uncertain conditions [4], [5]. Previous studies have shown that fuzzy logic controllers can improve motor speed response, reduce overshoot, and maintain low steady-state error under variable load conditions, while comparative investigations have further demonstrated their superior transient performance, faster settling time, and greater robustness than conventional PID-based approaches under varying operating conditions [6]-[9]. In addition, hybrid approaches such as fuzzy PI and fuzzy-based PID autotuning have been investigated to improve dynamic response and steady-state stability in motor control applications [10]. Similar advantages have also been demonstrated in thermal management systems, where fuzzy logic based temperature regulation and cooling fan control provide smoother, more adaptive responses to changing thermal conditions than conventional on off or fixed linear control strategies. [11]-[14].

Despite the widespread application of fuzzy controllers in motor drives and thermal management, most studies primarily evaluate control performance rather than systematically analyzing the complete fuzzy rule base or the behavior of all rule combinations across the input space. Consequently, the operation of the fuzzy inference mechanism over the entire rule base is often not explicitly demonstrated [15], [16]. Therefore, this study performs a systematic simulation-based evaluation of all 81 fuzzy-rule combinations using an automated testing procedure. This approach ensures that every rule in the fuzzy rule base is activated and evaluated under representative operating conditions, which is rarely reported in previous studies.

Based on this gap, the objective of this research is to design and evaluate, through a GUI-based simulation environment, a fuzzy logic controller capable of maintaining the BLDC motor speed at the desired reference value while simultaneously regulating the cooling fan according to the motor temperature and its rate of change. The proposed controller is implemented in an interactive simulation platform equipped with visualization, data logging, and automated testing features, enabling systematic evaluation of the controller behavior prior to hardware implementation.

The primary contribution of this study is the development of a unified fuzzy control strategy that simultaneously regulates BLDC motor speed and cooling-fan operation while systematically evaluating all 81 fuzzy-rule combinations through an automated testing procedure. Unlike previous studies, which primarily focused on fuzzy controller design and rule-base optimization rather than comprehensive analysis of the complete fuzzy rule base, this work systematically investigates the behavior of all fuzzy rules over the entire input space within a GUI-based simulation environment before hardware implementation [17]. To realize this framework, the controller employs triangular membership functions, weighted-average defuzzification, and discrete PWM-to-RPM mapping to provide a computationally efficient approximation of actuator responses during simulation. A further contribution of this work is the implementation of a rule-aware automated testing procedure that activates every fuzzy rule and records the corresponding controller outputs for quantitative analysis. Consequently, this study provides theoretical insight into fuzzy-rule behavior and establishes a simulation-based foundation for future hardware implementation and experimental validation of integrated BLDC motor speed and thermal management systems.

2. METHODS

Figure 1 illustrates the closed-loop control architecture for the BLDC motor system. The motor speed reference RPM_{ref} is compared with the measured motor speed RPM_{meas} to generate the speed error.In discrete form, this error is defined as

$$e(k) = RPM_{ref}(k) - RPM_{meas}(k) \quad (1)$$

where:

- $e(k)$: speed error at the k-th sampling instant (rpm)
- $RPM_{ref}(k)$: reference motor speed (rpm)
- $RPM_{meas}(k)$: measured motor speed (rpm)
- k: discrete sampling index.

and the change of error is expressed as

$$\Delta e(k) = e(k) - e(k-1) \quad (2)$$

where:

- $\Delta e(k)$: change in speed error (rpm);
- $e(k)$: current speed error (rpm);
- $e(k-1)$: previous speed error (rpm).

The diagram also includes a cooling subsystem that monitors the motor temperature, resulting in a temperature error

$$e_T(k) = T_{ref}(k) - T_{meas}(k) \tag{3}$$

where :

- $e_T(k)$: motor temperature error at the k-th sampling instant (°C);
- $T_{ref}(k)$: reference motor temperature at the k-th sampling instant (°C);
- $T_{meas}(k)$: measured motor temperature at the k-th sampling instant (°C);

and the change of temperature error

$$\Delta e_T(k) = e_T(k) - e_T(k-1) \tag{4}$$

where:

- $\Delta e_T(k)$: change in temperature error (°C);
- $e_T(k)$: current temperature error (°C);
- $e_T(k-1)$: previous temperature error (°C).

These four variables $e(k)$, Δe(k), $e_T(k)$, and $\Delta e_T(k)$ serve as the primary inputs to the fuzzy controller, which regulates the PWM signals for both the motor and the cooling fan. The use of error and change-of-error as the primary inputs is a conventional design approach in fuzzy control systems [18].

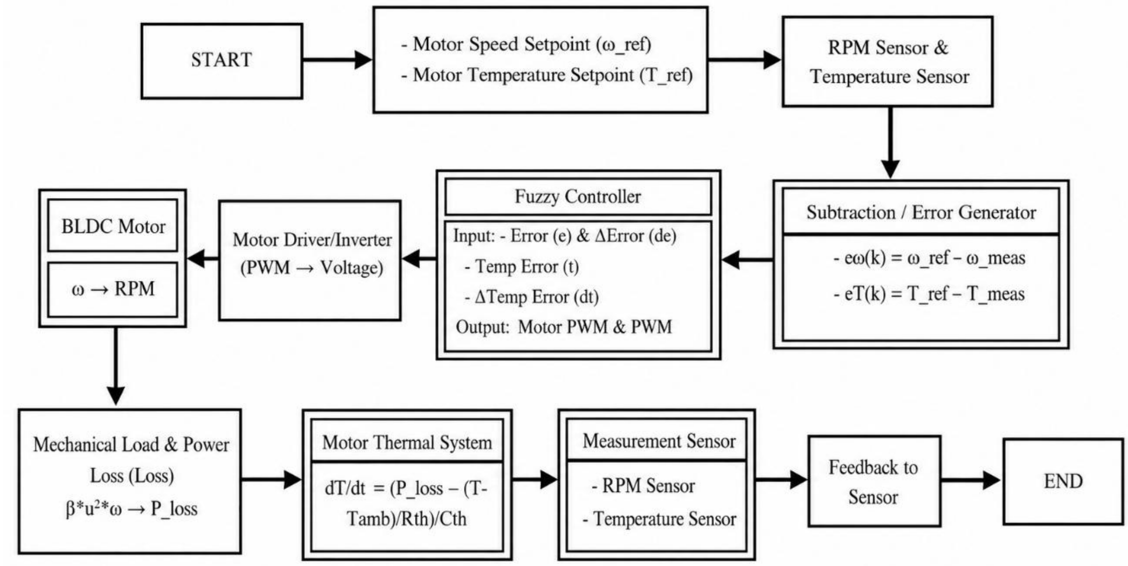

Figure 1. Flow Diagram of the 10 kW BLDC Motor Control System

The fuzzy controller structure is shown in Figure 2 and consists of fuzzification, rule evaluation, aggregation, and defuzzification. During fuzzification, each input is mapped to a triangular membership function, which is widely adopted because of its simplicity, computational efficiency, and ease of implementation in fuzzy control systems [18].

$$\mu_{tri}(x; a, b, c) = \max\left(\min\left(\frac{x-a}{b-a}, \frac{c-x}{c-b}\right), 0\right) \tag{5}$$

where:

- $\mu_{tri}(x)$: membership degree;
- x: input variable;
- a, b, c: triangular membership parameters.

where $a < b < c$, ensuring that both denominators remain non-zero. In the implementation, RPM error and Δe are represented by the linguistic sets NEG, ZERO, and POS, whereas temperature and Δe_T are represented by LOW, MED, and HIGH. The GUI displays these membership functions to help visualize the position of each input relative to its linguistic terms.

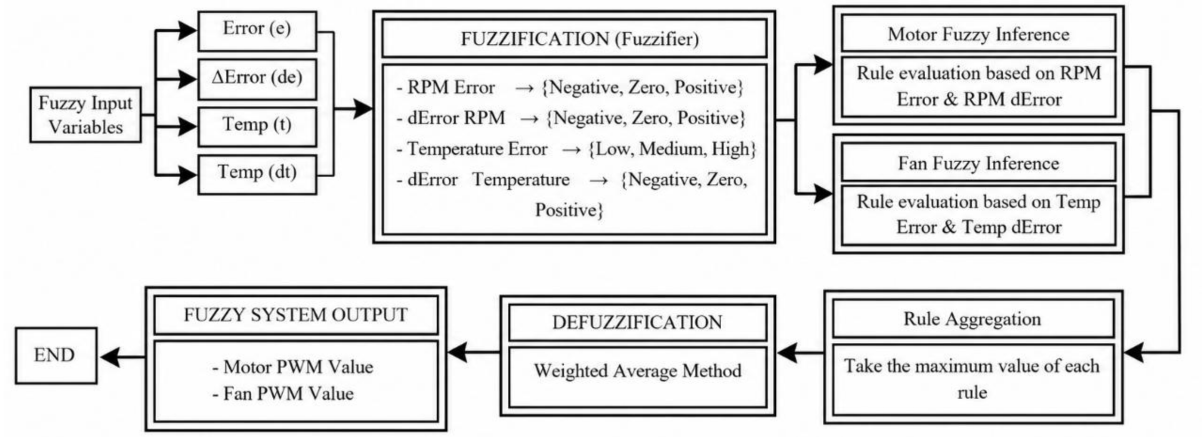

Figure 2. Fuzzy controller architecture for the BLDC motor control system illustrated in Fig. 1

Each fuzzy rule is expressed in IF–THEN form. The rule activation degree is computed using the minimum operator as

$$\alpha_i = \min(\mu_E^A, \mu_{\Delta E}^B, \mu_T^C, \mu_{\Delta T}^D) \tag{6}$$

where:

- α_i is the firing strength of the i-th fuzzy rule;
- μ_E^A is the membership degree of the speed error corresponding to the linguistic term A;
- $\mu_{\Delta E}^B$ is the membership degree of the change in speed error corresponding to the linguistic term B;
- μ_T^C is the membership degree of the temperature error corresponding to the linguistic term C;
- $\mu_{\Delta T}^D$ is the membership degree of the change in temperature error corresponding to the linguistic term D.

Equation (6) follows the conventional Mamdani fuzzy inference mechanism, where the logical AND operation is implemented using the minimum operator to determine the firing strength of each fuzzy rule [18].
The minimum operator is employed because each fuzzy rule represents the logical conjunction (AND) of the four antecedent conditions. Consequently, the firing strength of a rule is determined by its least satisfied antecedent, following the conventional Mamdani inference mechanism. The resulting activation degree is subsequently used during the defuzzification stage to compute the motor and cooling-fan PWM outputs.
The controller output is obtained using the weighted-average defuzzification method, which is commonly employed in singleton-based fuzzy inference systems because of its computational efficiency and smooth output generation [18].

$$PWM_m = \frac{\mu_e^- P_- + \mu_e^0 P_0 + \max(\mu_e^+, \mu_{\Delta e}^+) P_+}{\mu_e^- + \mu_e^0 + \max(\mu_e^+, \mu_{\Delta e}^+) + \varepsilon} \tag{7}$$

Where:

- PWM_m is the motor PWM output;
- μ_e^-, μ_e^0, and μ_e^+ are the membership degrees of the speed error corresponding to the NEG, ZERO, and POS linguistic sets, respectively;
- $\mu_{\Delta e}^+$ is the membership degree of the positive change in speed error;
- P_-, P_0, and P_+ are the singleton output weights for the LOW, MEDIUM, and HIGH motor PWM levels, respectively;
- ε is a small positive constant introduced to avoid division by zero.

Unlike the minimum operator used for antecedent evaluation in Equation (6), the maximum operator in Equation (7) is applied only during output aggregation. Multiple activated rules may support the same positive output singleton through either a positive speed error or a positive change in speed error. Therefore, the maximum operator preserves the strongest contribution without double-counting overlapping memberships. This simplified aggregation strategy reduces computational complexity while maintaining the intended control behavior, particularly the rapid acceleration response and thermal safety prioritization required by the controller. Accordingly, the antecedent evaluation remains based on the minimum operator defined in Equation (6), whereas the maximum operator is used exclusively for aggregating the contributions of rules that support the same output singleton.

Following the weighted-average defuzzification approach described in [18], the singleton output weights for the motor controller are assigned values of 100, 150, and 255, corresponding to the LOW, MEDIUM, and HIGH PWM levels, respectively. The cooling-fan output is computed using the same weighted-average defuzzification approach with temperature-related membership values and singleton output weights of 20, 80, and 255. Furthermore, the positive temperature-error change (Δe_T) is incorporated to detect rapid temperature increases, enabling the controller to increase the fan speed promptly whenever thermal safety becomes a priority. After defuzzification, the PWM values are converted into actuator responses using a piecewise PWM-to-RPM model. The motor output is mapped to discrete RPM levels (e.g., 0, 250, 400, 800, ..., up to 5000 rpm). Similarly, the cooling fan uses a duty-cycle conversion,

$$Duty = \frac{PWM}{255} \times 100\% \tag{8}$$

Where:

- Duty : PWM duty cycle (%)
- PWM : pulse width modulation value (0–255)

together with a lookup table relating duty cycle to fan RPM. This discrete approximation represents the actuator behavior without requiring a continuous physical model and facilitates systematic evaluation of the fuzzy rule base in the GUI prior to future hardware implementation.

The fuzzy rule base contains 81 combinations derived from the four inputs, each having three linguistic sets. For presentation efficiency, Tables 1–3 show compact 3×3 representations for the temperature conditions LOW, MED, and HIGH. Each cell contains three ordered tuples of (PWM_{motor}, PWM_{fan})corresponding to ΔT = NEG, ZERO, and POS, respectively. Thus, the ordering inside each cell is explicitly read from left to right as ΔT =NEG, ΔT = ZERO, and ΔT = POS.

At low temperatures, cooling is not prioritized; thus, fuzzy rules keep the fan PWM at low to medium levels unless a rapid temperature rise (ΔT > 0) occurs. Motor PWM control is mainly governed by speed error and its change. Table 1 lists the 27 fuzzy rules for the T = "LOW" condition.

Table 1. Design of fuzzy rules to maintain the cooling fan PWM at low to medium levels (compact 3×3 representation).

E \ ΔE	NEG	ZERO	POS
NEG	(100,20);(100,20);(100,80)	(100,20);(100,20);(100,80)	(150,20);(150,20);(150,80)
ZERO	(150,20);(150,20);(150,80)	(150,20);(150,20);(150,80)	(255,20);(255,20);(255,80)
POS	(255,20);(255,20);(255,80)	(255,20);(255,20);(255,80)	(255,20);(255,20);(255,80)

Note : Each cell contains three tuples for ΔT = NEG ; ZERO ; POS in that order, formatted as (PWM_motor,PWM_fan). Rows = E ∈ {NEG, ZERO, POS}; columns = ΔE ∈ {NEG, ZERO, POS}.

At medium temperatures, cooling becomes more important, the fan PWM is typically set to a medium level and increases when a temperature rise (ΔT > 0) is detected. Motor PWM control remains governed by the speed error and its change. Table 2 lists the 27 fuzzy rules for T = "MED".

Table 2. Design of fuzzy rules to maintain the cooling fan PWM at a medium level (compact 3×3 representation).

E\ΔE	NEG	ZERO	POS
NEG	(100,80);(100,80);(100,255)	(100,80);(100,80);(100,255)	(150,80);(150,80);(150,255)
ZERO	(150,80);(150,80);(150,255)	(150,80);(150,80);(150,255)	(255,80);(255,80);(255,255)
POS	(255,80);(255,80);(255,255)	(255,80);(255,80);(255,255)	(255,80);(255,80);(255,255)

Note : Cell format and ordering are identical to Table 1.
At high temperatures, thermal safety is prioritized, all rules set the fan PWM to its maximum regardless of speed error or its change, while motor PWM remains regulated by speed error to maintain performance. Table 3 lists the 27 fuzzy rules for T = "HIGH".

Table 3. Design of fuzzy rules to maintain the cooling fan PWM at a high level (compact 3×3 representation).

E\ΔE	NEG	ZERO	POS
NEG	(100,255);(100,255);(100,255)	(100,255);(100,255);(100,255)	(150,255);(150,255);(150,255)
ZERO	(150,255);(150,255);(150,255)	(150,255);(150,255);(150,255)	(255,255);(255,255);(255,255)
POS	(255,255);(255,255);(255,255)	(255,255);(255,255);(255,255)	(255,255);(255,255);(255,255)

Note : Cell format and ordering are identical to Table 1.
The fuzzy rule base comprises 81 rules spanning all combinations of the speed and temperature input variables. Each rule contributes to the final control action through its firing strength, as defined in Equation (6), and the weighted-average defuzzification process in Equation (7). This rule structure is consistent with the fuzzy inference architecture illustrated in Fig. 2 while employing the simplified output aggregation strategy described previously to improve computational efficiency for real-time implementation.

Due to space limitations, Tables 1–3 present representative subsets of the rule base using compact 3 × 3 matrices for the LOW, MED, and HIGH temperature conditions. The complete 81-rule table, listing all combinations of the input variables (E, ΔE, T, and ΔT) together with the corresponding motor and fan PWM outputs, is provided in Appendix A. This appendix ensures the reproducibility of the proposed fuzzy controller while keeping the main manuscript concise.

The proposed fuzzy controller was implemented in a Python-based graphical user interface (GUI) developed using Tkinter and the scikit-fuzzy library. The GUI provides interactive input controls, visualization of the membership functions, automatic computation of motor and cooling-fan PWM outputs, data logging, Excel/CSV export, and an automated testing module. This platform serves as the simulation environment used to evaluate the controller behavior before future hardware implementation.

The automated testing procedure systematically evaluates all 81 unique fuzzy-rule combinations derived from the four input variables, each represented by three linguistic sets ($3^4 = 81$). Each rule combination is evaluated once to ensure that every fuzzy rule in the rule base is activated. For each evaluation, the corresponding motor and cooling-fan PWM outputs are computed and recorded automatically. The recorded outputs are then exported for subsequent quantitative analysis and verification of the controller behavior across the complete input space.

3. RESULTS AND DISCUSSION

Simulation experiments were conducted to evaluate the fuzzy controller described in Section 2. The controller was tested using the four fuzzy inputs (E, ΔE, ET, and ΔET), while the motor PWM/RPM and fan PWM/RPM served as the controller outputs. The automated testing procedure generated results for all 81 unique fuzzy-rule combinations. Table 4 presents 36 representative samples selected to illustrate the controller behavior over different operating conditions, while the complete dataset was used for the quantitative analysis reported later in this section. These samples provide a representative basis for evaluating the effects of the fuzzification, inference, and defuzzification processes on the actuator responses.

Table 4. Experimental results for the BLDC motor fuzzy control system under 36 test conditions

No.	Speed Level	Reference RPM	Temperature (°C)	RPM Error (rpm)	ΔRPM Error (rpm)	Temperature Error (°C)	ΔTemperature Error (°C)	Motor PWM	Motor RPM	Fan PWM	Fan RPM
1	8	5000	26.86	-723.25	208.1	33.14	-18.76	10	196	28.2	1380
2	5	2000	43.06	-1061.4	-72.98	16.94	9.3	10	196	38.3	1879
3	8	5000	117.77	1604.34	-498.79	-57.77	-3.27	16.4	320	255	4500
4	3	800	48.9	-1294.65	27.82	11.1	11.47	10	196	88.1	3081
5	1	200	86.01	-221.71	242.09	-26.01	-2.08	16.7	327	100.3	3272
6	4	1000	33.24	1400.04	-158.03	26.76	-18.02	178.5	3500	22.7	1114
7	2	400	39.74	1175.46	-197.32	20.26	0.93	149.9	2938	20.3	993

8	2	400	73.2	1610.27	393.65	-13.2	-5.32	154.0	3019	94.7	3185
9	6	3000	102.42	-306.57	-215.0	-42.42	2.21	10	196	255	4500
10	2	400	68.08	-592.26	475.24	-8.08	-4.8	10	196	102.3	3302
11	5	2000	29.41	-1293.43	-147.8	30.59	19.36	10	196	36.7	1799
12	1	200	50.91	-1421.15	-190.88	9.09	-14.78	10	196	72.7	2839
13	3	800	49.56	167.94	-90.64	10.44	14.2	81.2	1591	92.8	3155
14	8	5000	115.11	119.98	73.8	-55.11	-16.71	16.7	328	255	4500
15	7	4000	58.15	341.26	-437.68	1.85	15.24	87.4	1713	154.7	3820
16	1	200	118.57	-293.6	-50.39	-58.57	-6.79	10	196	255	4500
17	3	800	114.58	708.73	-82.19	-54.58	-3.21	10	196	255	4500
18	2	400	112.18	1754.16	-123.58	-52.18	10.8	17.9	350	255	4500
19	8	5000	91.19	-1476.93	344.49	-31.19	-2.48	10	196	255	4500
20	3	800	55.04	-245.6	-176.46	4.96	19.05	34.3	673	132.3	3556
21	6	3000	95.44	1053.7	233.03	-35.44	-10.18	53.7	1053	255	4500
22	3	800	57.53	-759.33	98.03	2.47	-2.14	10	196	125.2	3481
23	3	800	101.68	-1784.47	61.71	-41.68	17.24	10	196	255	4500
24	7	4000	112.47	558.84	298.63	-52.47	-4.0	10	196	255	4500
25	4	1000	91.71	-1321.91	389.16	-31.71	-0.27	10	196	255	4500
26	6	3000	114.33	27.53	27.49	-54.33	2.25	15.4	301	255	4500
27	2	400	38.32	-801.59	-134.25	21.68	-18.67	10	196	18.4	903
28	8	5000	95.42	-1271.36	-391.18	-35.42	3.29	10	196	255	4500
29	1	200	114.74	-1349.31	-56.68	-54.74	-10.05	10	196	255	4500
30	3	800	32.36	-685.63	458.56	27.64	12.86	10	196	33.2	1626
31	5	2000	46.31	-1322.83	18.3	13.69	-3.23	10	196	57.9	2607
32	7	4000	89.55	391.11	-118.43	-29.55	-4.8	100.0	1959	101.8	3296
33	5	2000	46.53	138.23	206.69	13.47	-6.52	133.4	2615	59.2	2628
34	1	200	112.12	1492.58	-328.24	-52.12	-0.49	15.2	298	255	4500
35	6	3000	117.51	952.49	-207.45	-57.51	-12.17	10	196	255	4500
36	8	5000	22.31	1549.72	487.29	37.69	1.3	197.6	3874	37.7	1847

Note: *Speed Level* is a categorical test setting representing the reference speed condition, where 1 = 250 rpm, 2 = 400 rpm, 3 = 800 rpm, 4 = 1000 rpm, 5 = 2000 rpm, and 6 = 3000 rpm. RPM Error and ΔRPM Error are expressed in rpm, while Temperature Error and ΔTemperature Error are expressed in °C.

The membership-function plots (Fig. 3) show that many measurements lie in transition regions between linguistic labels (e.g., NEG/ZERO or ZERO/POS for RPM error and LOW/MED/HIGH for temperature). Due to the overlapping triangular functions, multiple rules are partially activated, producing intermediate PWM outputs. This is reflected in the experimental results, where motor PWM values cluster around 100–150 and fan PWM around 20–80 before sharply increasing to 200–255 under strong HIGH or positive ΔTactivation, consistent with the fuzzification and aggregation design in Section 2.

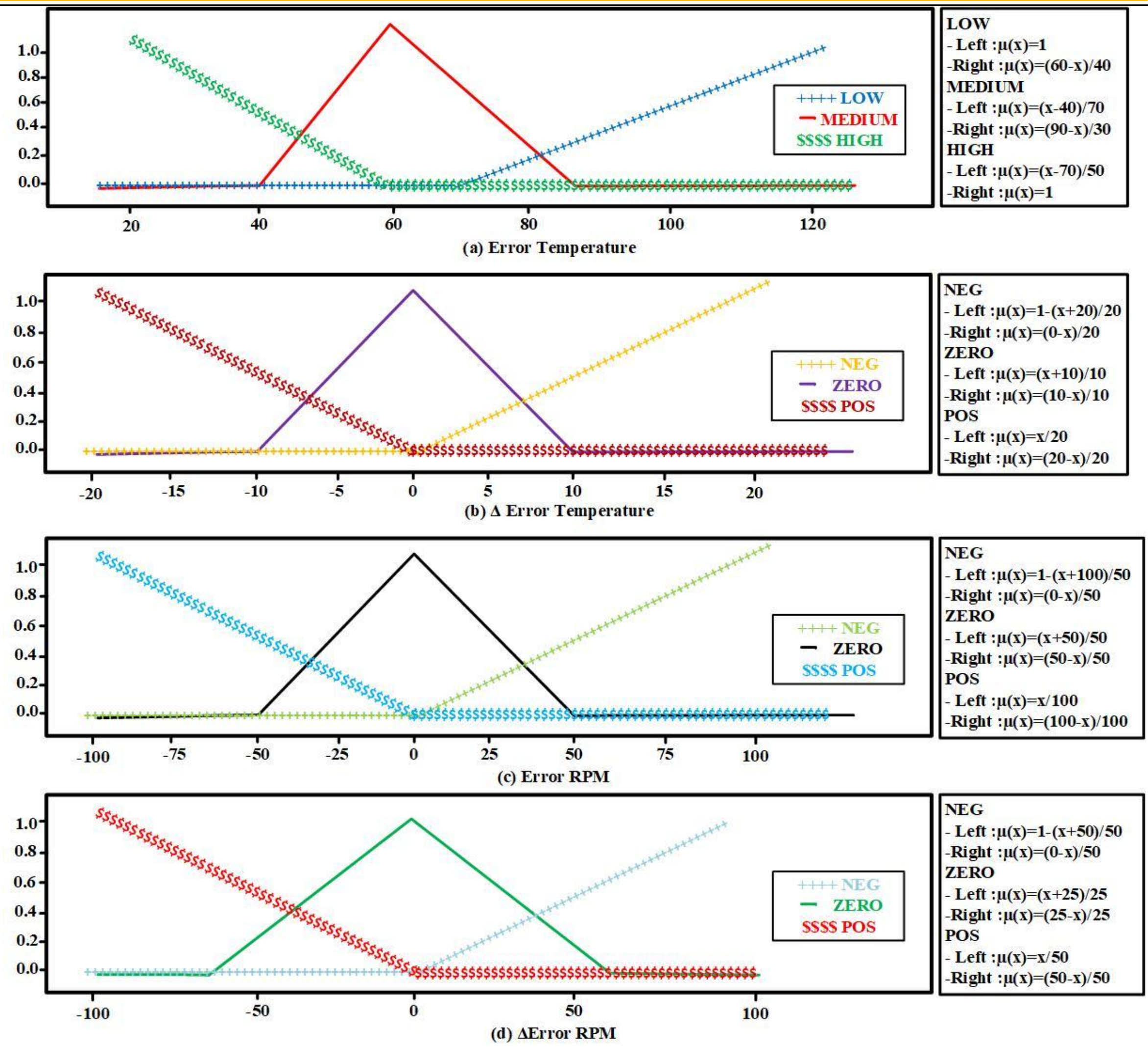

Figure 3. Membership function plots

The representative samples shown in Table 4 and the complete dataset of 81 fuzzy-rule combinations consistently demonstrate the expected relationship between RPM error and motor PWM: large positive RPM errors (≈ +90) produce high motor PWM values (≈ 200–230) and mapped motor speeds of about 4300–4500 rpm, indicating acceleration demand. In contrast, negative or small RPM errors yield lower PWM outputs (≈ 30–150) with mapped motor speeds between 250 and 3300 rpm. This behavior verifies that the motor-control rules based on the combined effects of $E$and ΔE operate as intended.

The effect of error dynamics ΔE is evident in transient cases where the RPM error is moderate but increasing. Samples with $E \approx 40$ and positive ΔE show higher motor PWM outputs (≈110–200, mapped to 3800–4300 rpm) than cases with similar E but negative ΔE, which yield lower PWM values (≈20–80, mapped to 2500–3300 rpm). This confirms that including ΔE in the rule base effectively captures the need for rapid corrective acceleration, as defined in the methodology.

Cooling-system results show consistent application of thermal safety rules: samples with HIGH temperature error or positive ΔE_T produce maximum fan PWM (255) and mapped speeds of 4300–4500 rpm. At LOW or MED temperatures, fan PWM typically remains within 20–80, unless a positive ΔE_T raises it to about 110–200 (≈3800 rpm), demonstrating that the temperature rise rate alone can trigger strong cooling. This confirms the effectiveness of the max operator and priority rules in the rule base.

The discrete PWM–RPM mapping must be considered when interpreting the results, as PWM values are assigned to RPM buckets (e.g., low PWM → 250–400 rpm, medium → 800–2000 rpm, high → 3000–5000 rpm). As a result, small PWM changes may cause stepwise jumps rather than proportional RPM variations; for example, PWM ≈30 maps to 250 rpm, ≈200 to 3000 rpm, and ≈230 to 4500 rpm. Therefore, quantitative PWM–RPM analysis should account for this stepwise behavior.

The results show that the optimized implementation, which employs weighted-average defuzzification instead of conventional centroid defuzzification while retaining the complete 81-rule fuzzy rule base, preserves the intended control behavior. These include thermal safety prioritization, sensitivity to ΔE for rapid correction, and averaging effects from partial rule activation. The observed motor and fan PWM patterns and mapped RPMs are therefore theoretically consistent with the rule base, while intermediate outputs are explained by membership overlap and weighted-average defuzzification, which combines the contributions of multiple activated rules.

Since this study is simulation-based, the observed inaccuracies mainly arise from the discretization of the input variables, the simplified weighted-average defuzzification process, and the discrete PWM-to-RPM mapping rather than from physical sensor noise. The weighted-average defuzzification attenuates small input variations, while the discrete PWM-to-RPM mapping produces stepwise changes in the actuator response (e.g., a fan PWM increase from approximately 80 to 137 results in a speed transition from about 3300 rpm to 3800 rpm). In addition, further refinement of the membership functions may improve the resolution and linearity of the controller outputs, providing a useful direction for future hardware implementation.

An additional limitation of this study is that the controller evaluation is restricted to simulation-based analysis and therefore does not include standard real-time control performance metrics such as rise time, settling time, overshoot, or steady-state response under actual hardware operation. These metrics generally require closed-loop experimental validation using a physical BLDC motor system and cannot be reliably assessed within the simplified GUI-based simulation environment employed in this work. Consequently, the present study focuses on verifying the correctness of the fuzzy inference mechanism, the complete 81-rule base, and the corresponding actuator responses rather than evaluating dynamic real-time performance. Experimental validation incorporating these standard control-performance metrics will therefore constitute an important direction for future research.

To complement the qualitative observations discussed above, descriptive statistics were computed using all 81 unique fuzzy-rule combinations. The results are summarized in Table 5.

Table 5. Descriptive statistics of motor and fan outputs obtained from the 81 unique fuzzy-rule combinations

RPM Error Range	Samples	Mean Motor PWM	SD Motor PWM	Mean Motor RPM	SD Motor RPM	Mean Fan PWM	SD Fan PWM
−100 to −50	23	30.0000	0.0000	196.0000	0.0000	137.8870	95.5449
−50 to 0	30	56.7200	55.7913	1111.8333	1093.9446	126.4433	84.2407
0 to 50	16	68.4625	53.8964	1342.1250	1056.6828	166.9563	85.3842
50 to 100	12	151.8083	61.3095	2976.0000	1202.3335	137.4167	75.2883

Note: Mean Motor RPM and Mean Fan RPM represent the actuator speeds obtained from the PWM-to-RPM mapping used in the GUI-based fuzzy controller simulation.

To complement the representative samples presented in Table 4, descriptive statistics were computed using all 81 unique fuzzy-rule combinations, as summarized in Table 5. The results show that motor PWM increases with increasing RPM error. For large negative RPM errors (−100 to −50), the motor PWM remains constant at 30.00 (SD = 0.00), indicating that all corresponding fuzzy rules generate the same low control action. As the RPM error increases, the average motor PWM also increases, reaching 151.81 for the 50 to 100 range. The larger standard deviations in the remaining ranges indicate the influence of overlapping membership functions and weighted-average defuzzification, which produce intermediate PWM values through simultaneous activation of multiple fuzzy rules. In contrast, the mean fan PWM remains relatively stable across all RPM error ranges because it is primarily determined by the temperature error and its rate of change. Overall, these statistical results quantitatively confirm the expected behavior of the proposed fuzzy controller and are consistent with the qualitative observations obtained from the representative samples in Table 4.

4. CONCLUSION

This study presented a simulation-based fuzzy logic controller that integrates BLDC motor speed control and thermal management within a unified control framework. The controller employs four fuzzy inputs with three linguistic sets each, resulting in 81 fuzzy rules that were systematically evaluated using an automated testing procedure. The simulation results confirm that all rule combinations were successfully activated and that the controller produces stable and adaptive motor and cooling-fan PWM outputs consistent with the designed fuzzy-rule base.

The primary limitation of this study is that the evaluation was conducted entirely in a GUI-based simulation environment without real-hardware implementation or closed-loop time-series measurements.

Consequently, dynamic performance metrics such as rise time, settling time, overshoot, MAE, and RMSE cannot be computed from the available dataset because the simulation evaluates independent fuzzy-rule combinations rather than transient system responses. Future work will therefore focus on implementing the proposed controller on an actual BLDC motor platform to enable comprehensive experimental validation and comparison with conventional controllers such as PID.

5. ACKNOWLEDGEMENT
The authors would like to express their gratitude to the Faculty of Engineering, University of Garut, and the Telecommunications Research Center, National Research and Innovation Agency (BRIN), for providing the facilities and infrastructure that enabled this research to be conducted successfully.

6. REFERENCES
[1] R. Kristiyono and Wiyono, "Autotuning fuzzy PID controller for speed control of BLDC motor," *Journal of Robotics and Control (JRC)*, vol. 2, no. 5, pp. 400–407, Sep. 2021, doi: 10.18196/jrc.25114.
[2] S. GUNTAY and I. SARITAS, "BLDC Motor speed control with dynamic adjustment of PID coefficients: Comparison of fuzzy and classic PID," *International Journal of Applied Methods in Electronics and Computers*, vol. 12, no. 1, pp. 22–32, 2024, doi: 10.58190/ijamec.2024.80.
[3] S. M. Deshmukh and R. P. Mahobia, "BLDC Motor Speed Control with Digital Adaptive ANFIS and Reduced Harmonic Content," *Nanotechnol. Percept.*, vol. 20, no. S4, pp. 11–26, 2024, doi: 10.62441/nano-ntp.v20iS4.2.
[4] J. H. Kim and S. J. Oh, "A fuzzy PID controller for nonlinear and uncertain systems," *Soft comput.*, vol. 4, no. 2, pp. 123–129, 2000, doi: 10.1007/s005000000039.
[5] M. Braae and D. A. Rutherford, "Theoretical and linguistic aspects of the fuzzy logic controller," *Automatica*, vol. 15, no. 5, pp. 553–577, 1979, doi: https://doi.org/10.1016/0005-1098(79)90005-0.
[6] S. Sunardi, A. Yudhana, and F. Furizal, "Impact of Fuzzy Tsukamoto in Controlling Room Temperature and Humidity," *INTENSIF: Jurnal Ilmiah Penelitian dan Penerapan Teknologi Sistem Informasi*, vol. 7, no. 2, pp. 221–242, 2023, doi: 10.29407/intensif.v7i2.19652.
[7] Q.-H. Pham *et al.*, "Design of a Fuzzy Controller for a Heating Furnace System," *Indonesian Journal of Engineering and Science*, vol. 6, no. 2, pp. 125–135, 2025, doi: https://doi.org/10.51630/ijes.vx.xxx.
[8] E. Gowthaman, V. Vinodhini, M. Y. Hussain, S. K. Dhinakaran, and T. Sabarinathan, "Speed Control of Permanent Magnet Brushless DC Motor Using Hybrid Fuzzy Proportional plus Integral plus Derivative Controller," *Energy Procedia*, vol. 117, pp. 1101–1108, 2017, doi: 10.1016/j.egypro.2017.05.234.
[9] A. Varshney, D. Gupta, and B. Dwivedi, "Speed response of brushless DC motor using fuzzy PID controller under varying load condition," *Journal of Electrical Systems and Information Technology*, vol. 4, no. 2, pp. 310–321, 2017, doi: 10.1016/j.jesit.2016.12.014.
[10] N. A. Sulaiman, M. F. Othman, and H. Abdullah, "Fuzzy logic control of centralized chilled water system," *J. Teknol.*, vol. 72, no. 2, pp. 57–62, 2015, doi: 10.11113/jt.v72.3884.
[11] I. Soesanti and R. Syahputra, "A Fuzzy Logic Controller Approach for Controlling Heat Exchanger Temperature," *Journal of Electrical Technology UMY*, vol. 3, no. 4, pp. 117–124, 2019, doi: 10.18196/jet.3462.
[12] R. Bangun *et al.*, "RANCANG BANGUN KONTROLLER PENDINGIN UNTUK UNIT PELTIER BERBASIS FUZZY LOGIC Frima Setyawan Nur Rohman".
[13] H. Yan, Y. Pan, Z. Li, and S. Deng, "Further development of a thermal comfort based fuzzy logic controller for a direct expansion air conditioning system," *Appl. Energy*, vol. 219, pp. 312–324, 2018, doi: https://doi.org/10.1016/j.apenergy.2018.03.045.
[14] Y. Cui, W. Zhang, and B. He, "A Variation-Aware Adaptive Fuzzy Control System for Thermal Management of Microprocessors," *IEEE Trans. Very Large Scale Integr. VLSI Syst.*, vol. 25, no. 2, pp. 683–695, 2017, doi: 10.1109/TVLSI.2016.2596338.
[15] M. H. N. Talib *et al.*, "An improved simplified rules Fuzzy Logic Speed Controller method applied for induction motor drive," *ISA Trans.*, vol. 105, pp. 230–239, 2020, doi: https://doi.org/10.1016/j.isatra.2020.05.040.
[16] N. Öztürk and E. Çelik, "Speed control of permanent magnet synchronous motors using fuzzy controller based on genetic algorithms," *International Journal of Electrical Power & Energy Systems*, vol. 43, no. 1, pp. 889–898, 2012, doi: https://doi.org/10.1016/j.ijepes.2012.06.013.
[17] K. Belarbi, F. Titel, W. Bourebia, and K. Benmahammed, "Design of Mamdani fuzzy logic controllers with rule base minimisation using genetic algorithm," *Eng. Appl. Artif. Intell.*, vol. 18, no. 7, pp. 875–880, 2005, doi: https://doi.org/10.1016/j.engappai.2005.03.003.

[18] T. J. Ross, *Fuzzy Logic with Engineering Applications*. Wiley, 2016. [Online]. Available: https://books.google.co.id/books?id=ijsbDQAAQBAJ

APPENDIX A

Appendix A presents the complete fuzzy rule base consisting of all 81 rule combinations generated from the four fuzzy input variables (E, ΔE, T, and ΔT). Each rule specifies the corresponding singleton outputs for the motor PWM and cooling-fan PWM used by the proposed fuzzy inference system.

Table A1. Complete 81-Rule Base of the Proposed Fuzzy Controller

Rule No	RPM Error (E)	Change in RPM Error (ΔE)	Temperature Level (T)	Change in Temperature (ΔT)	Motor PWM	Cooling Fan PWM
1	NEG	NEG	LOW	NEG	100	20
2	NEG	NEG	LOW	ZERO	100	20
3	NEG	NEG	LOW	POS	100	80
4	NEG	ZERO	LOW	NEG	100	20
5	NEG	ZERO	LOW	ZERO	100	20
6	NEG	ZERO	LOW	POS	100	80
7	NEG	POS	LOW	NEG	150	20
8	NEG	POS	LOW	ZERO	150	20
9	NEG	POS	LOW	POS	150	80
10	ZERO	NEG	LOW	NEG	150	20
11	ZERO	NEG	LOW	ZERO	150	20
12	ZERO	NEG	LOW	POS	150	80
13	ZERO	ZERO	LOW	NEG	150	20
14	ZERO	ZERO	LOW	ZERO	150	20
15	ZERO	ZERO	LOW	POS	150	80
16	ZERO	POS	LOW	NEG	255	20
17	ZERO	POS	LOW	ZERO	255	20
18	ZERO	POS	LOW	POS	255	80
19	POS	NEG	LOW	NEG	255	20
20	POS	NEG	LOW	ZERO	255	20
21	POS	NEG	LOW	POS	255	80
22	POS	ZERO	LOW	NEG	255	20
23	POS	ZERO	LOW	ZERO	255	20
24	POS	ZERO	LOW	POS	255	80
25	POS	POS	LOW	NEG	255	20
26	POS	POS	LOW	ZERO	255	20
27	POS	POS	LOW	POS	255	80
28	NEG	NEG	MED	NEG	100	80
29	NEG	NEG	MED	ZERO	100	80
30	NEG	NEG	MED	POS	100	255
31	NEG	ZERO	MED	NEG	100	80
32	NEG	ZERO	MED	ZERO	100	80
33	NEG	ZERO	MED	POS	100	255
34	NEG	POS	MED	NEG	150	80
35	NEG	POS	MED	ZERO	150	80
36	NEG	POS	MED	POS	150	255
37	ZERO	NEG	MED	NEG	150	80

38	ZERO	NEG	MED	ZERO	150	80
39	ZERO	NEG	MED	POS	150	255
40	ZERO	ZERO	MED	NEG	150	80
41	ZERO	ZERO	MED	ZERO	150	80
42	ZERO	ZERO	MED	POS	150	255
43	ZERO	POS	MED	NEG	255	80
44	ZERO	POS	MED	ZERO	255	80
45	ZERO	POS	MED	POS	255	255
46	POS	NEG	MED	NEG	255	80
47	POS	NEG	MED	ZERO	255	80
48	POS	NEG	MED	POS	255	255
49	POS	ZERO	MED	NEG	255	80
50	POS	ZERO	MED	ZERO	255	80
51	POS	ZERO	MED	POS	255	255
52	POS	POS	MED	NEG	255	80
53	POS	POS	MED	ZERO	255	80
54	POS	POS	MED	POS	255	255
55	NEG	NEG	HIGH	NEG	100	255
56	NEG	NEG	HIGH	ZERO	100	255
57	NEG	NEG	HIGH	POS	100	255
58	NEG	ZERO	HIGH	NEG	100	255
59	NEG	ZERO	HIGH	ZERO	100	255
60	NEG	ZERO	HIGH	POS	100	255
61	NEG	POS	HIGH	NEG	150	255
62	NEG	POS	HIGH	ZERO	150	255
63	NEG	POS	HIGH	POS	150	255
64	ZERO	NEG	HIGH	NEG	150	255
65	ZERO	NEG	HIGH	ZERO	150	255
66	ZERO	NEG	HIGH	POS	150	255
67	ZERO	ZERO	HIGH	NEG	150	255
68	ZERO	ZERO	HIGH	ZERO	150	255
69	ZERO	ZERO	HIGH	POS	150	255
70	ZERO	POS	HIGH	NEG	255	255
71	ZERO	POS	HIGH	ZERO	255	255
72	ZERO	POS	HIGH	POS	255	255
73	POS	NEG	HIGH	NEG	255	255
74	POS	NEG	HIGH	ZERO	255	255
75	POS	NEG	HIGH	POS	255	255
76	POS	ZERO	HIGH	NEG	255	255
77	POS	ZERO	HIGH	ZERO	255	255
78	POS	ZERO	HIGH	POS	255	255
79	POS	POS	HIGH	NEG	255	255
80	POS	POS	HIGH	ZERO	255	255
81	POS	POS	HIGH	POS	255	255